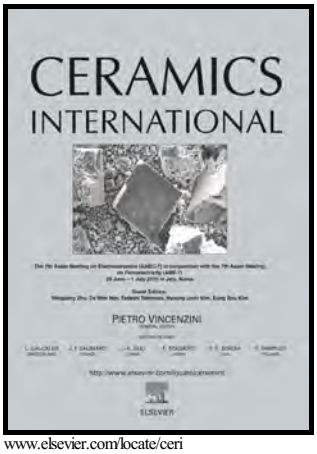

www.elsevier.com/locate/ceri

Temperature Stable and High-Q Microwave Dielectric Ceramics in the $Li_2Mg_{3-x}Ca_xTiO_6$system (x=0.00~0.18)

Zixuan Fang, Bin Tang, Feng Si, Shuren Zhang

PII: S0272-8842(16)31363-3
DOI: http://dx.doi.org/10.1016/j.ceramint.2016.08.055
Reference: CERI13507

To appear in: *Ceramics International*

Received date: 8 July 2016
Revised date: 6 August 2016
Accepted date: 8 August 2016

Cite this article as: Zixuan Fang, Bin Tang, Feng Si and Shuren Zhang Temperature Stable and High-Q Microwave Dielectric Ceramics in th $Li_2Mg_{3-x}Ca_xTiO_6$system (x=0.00~0.18), *Ceramics Internationa* http://dx.doi.org/10.1016/j.ceramint.2016.08.055

Temperature Stable and High-Q Microwave Dielectric Ceramics in the $Li_2Mg_{3-x}Ca_xTiO_6$ system (x=0.00~0.18)

Zixuan Fang[a,b], Bin Tang[a,b*], Feng Si[a,b], Shuren Zhang[a,b]

[a]National Engineering Center of Electromagnetic Radiation Control Materials,
University of Electronic Science and Technology of China, Jianshe Road, Chengdu 610054, PR China

[b]State Key Laboratory of Electronic Thin Films and Integrated Devices,
University of Electronic Science and Technology of China, Jianshe Road, Chengdu 610054, PR China

*tangbin@uestc.edu.cn

Abstract

Microwave dielectric properties of $Li_2Mg_{3-x}Ca_xTiO_6$ (x=0~0.18) ceramics were studied using a conventional solid-state route to find temperature stable and high Q microwave ceramics. As the calcination temperature was 500 °C, the Li_2TiO_3 phase with monoclinic rock salt structure in C2/c space group started to form. When the samples were calcined from 600 °C to 900 °C, the XRD patterns exhibited a remarkable chemical reaction between the MgO and Li_2TiO_3 phases, which eventually formed the $Li_2Mg_3TiO_6$ phase. The results indicated the $Li_2Mg_3TiO_6$ and $CaTiO_3$ co-existed with each other and formed a stable composite system when the calcium content was added. The SEM photographs indicated that the pores caused by the Li evaporation could be effectively reduced due to the appearance of $CaTiO_3$. As x was increased from 0 to 0.18, the relative density was significantly improved due to the elimination of pores. As the Ca content increased, the dielectric constant (ε_r) increased from 14.8 to 20.6; the quality factor ($Q\times f$) decreased from 148,713 GHz to 79,845 GHz, and the temperature coefficient of resonant frequency (τ_f) significantly increased from −42.4 to +10.8 ppm/°C due to the increased amount of $CaTiO_3$. Therefore, at x=0.12, the LMCxT ceramics sintered at 1280 °C for 6 h displayed excellent comprehensive properties of ε_r= 17.8, $Q\times f$= 102,246 GHz and τ_f= -0.7 ppm/°C.

Keywords: Microwave Ceramics; Dielectrics; Temperature Stable; High Q

1. Introduction

With the operating frequency of mobile telecommunications expanding to the microwave range, microwave dielectric ceramics have attracted increasing interest as key components of the filter, oscillator and antenna in the applications ranging from cellular phones to the global positioning system [1, 2]. Microwave dielectric materials have numerous advantages in terms of compactness, light weight, temperature stability and low production costs in high frequency devices. The search for microwave dielectric ceramics with a high quality factor ($Q\times f \geq 100,000$GHz), proper dielectric constant (ε_r), and near-zero temperature coefficient of the resonant frequency (τ_f) has always been an active field because of their essential roles in the wireless communication industry [3].

Recently, many Li containing dielectric materials, such as Li_2WO_4[4], Li_2MO_3 (M=Ti, Zr, Sn) [5] , $Li_2O–Bi_2O_3–MoO_3$[6], $Li_2ATi_3O_8$ (A=Mg or Zn)[7], $Li_3Mg_2NbO_6$ [8] and $Li_2Mg_3BO_6$ (B=Ti, Sn or Zr) [9, 10], have been the focus of microwave ceramics due to their excellent microwave dielectric properties. Among these excellent materials, the newly reported $Li_2Mg_3TiO_6$ with a face-centered cubic rock salt structure is a promising candidate in critical components of a microwave circuit system due to its excellent properties of ε_r =15.2, $Q\times f$ =152,000 GHz, and τ_f= -39 ppm/°C [9]. To date, only a small number of papers have reported their basic information, such as microwave properties and crystal structures [9-11]. Similar to many Li containing ceramics [12, 13], however, the porous microstructure caused by the evaporation of Li elements is detrimental for $Li_2Mg_3TiO_6$ to be used as resonator materials. Furthermore, the large negative τ_f of -39 ppm/°C makes it quite unstable at microwave frequencies. It is reported that addition of low sintering temperature additives can lower the sintering temperature; therefore, the evaporation of Li contents will be relieved to a certain extent, but this will seriously damage the microwave dielectric properties, especially ε_r and τ_f values [14, 15], and it also

complicates the synthesizing process, leading to the rising cost of mass production [7].

Fortunately, it has been demonstrated that an effective approach is to introduce a stable phase with a positive τ_f value in the synthesizing process. For example, Li et al.[13] reported that extra TiO_2 in $Li_2ZnTi_{3+x}O_{8+2x}$ ceramics would effectively eliminate the pores and tune the τ_f to zero because of the appearance of a TiO_2 phase. George et al.[7] revealed that introduction of a $CaTiO_3$ phase would enhance comprehensive microwave properties by improving porous microstructure and micro-cracks in $Li_2A_{1-x}Ca_xTi_3O_8$ ceramics. Thus, these methods make it possible to solve two critical issues for $Li_2Mg_3TiO_6$ ceramics. As a result, the effects of Ca-substitution for Mg on the sintering behaviors, phase structures, microstructures and the microwave dielectric properties of $Li_2Mg_{3-x}Ca_xTiO_6$ were investigated in detail in this paper.

2. Experimental Procedure

To prepare the $Li_2Mg_{3-x}Ca_xTiO_6$ and $Li_2Mg_{3-x}TiO_6$ powders, the starting raw materials were $Mg(OH)_2{\cdot}4MgCO_3{\cdot}5H_2O$, Li_2CO_3, $CaCO_3$ and TiO_2 with at least 99.0% purity. The powders were weighed as $Li_2Mg_{3-x}Ca_xTiO_6$ (LMCxT) and $Li_2Mg_{3-x}TiO_6$, where x =0.00, 0.03, 0.04, 0.06, 0.09, 0.12, 0.15 and 0.18, and were ball milled in a nylon jar with zirconia balls in ethanol for 7 h. The resulting mixtures were dried and calcined at 1000 °C for 4 h. Subsequently, the calcined powders were reground for 5 h, dried, mixed with a 6 wt% of a 10% solution of polyvinyl alcohol (PVA) as a binder and granulated. The obtained powder was axially pressed into cylindrical disks with a thickness of 7.5 mm and a diameter of 15 mm under a pressure of 200 kg/cm^2. The pellets of $Li_2Mg_{3-x}Ca_xTiO_6$ (LMCxT) were sintered at 1205°C, 1230 °C, 1255 °C, 1280 °C, 1305 °C and 1330 °C for 6 h in air with a temperature-ramp rate of 6 °C/min. And pellets of $Li_2Mg_{3-x}TiO_6$ (x=0.04, 0.12, 0.18) were sintered at 1280 °C for 6 h in air with a temperature-ramp rate of 6 °C/min.

After sintering, the apparent densities of the samples were measured using the Archimedes' method. The powder phase composition was examined by X-ray diffraction (XRD) using CuKα radiation (Philips x'pert Pro MPD, Netherlands). Scanning electron microscopy (SEM) (FEI Inspect F, United Kingdom) coupled with energy dispersive X-ray spectroscopy (EDX) was employed to study the thermally etched surface morphology of the specimens. The dielectric characteristics at microwave frequencies were measured by the Hakki–Coleman dielectric resonator method in the TE011 mode using a network analyzer (Agilent Technologies E5071C, USA) and temperature chamber (DELTA 9023, Delta Design, USA). The temperature coefficients of resonant frequency measured at 7~9 GHz were calculated by the equation: $\tau_f = \left(f_{t_2} - f_{t_1} \right) / \left(f_{t_1} \times \left(t_2 - t_1 \right) \right)$ (1), where f_{t_1} and f_{t_2} are the resonant frequencies at the measuring temperature t_1 (25 °C) and t_2 (85 °C) respectively.

3. Results and Discussion

Fig. 1(a)~(i) shows the XRD patterns of LMCxT (x=0.12) powders calcined at 400 °C~1200 °C for 4 h in air. When the calcination temperature was 400 °C, raw TiO_2 (JPCDS# 65-1118), Li_2CO_3 (JPCDS#87-0728) and $CaCO_3$ (JPCDS#86-2334) were observed, and newly formed MgO (JPCDS#89-7746) was also detected. While the calcination temperature was 500 °C, the Li_2TiO_3 (JPCDS#33-0831) with monoclinic rock salt structure in C2/c space group started to form, and the CaO (JPCDS#78-0649) was obtained for the first time. As the calcination temperature was 600 °C, the intensity of Li_2TiO_3 phase became stronger, but the Li_2CO_3 and $CaCO_3$ phase disappeared completely. When the calcination temperature was increased to 800 °C, the intensity of MgO phase became weaker, but that of Li_2TiO_3 phase grew stronger and weak characteristic peaks of $CaTiO_3$ phase were detected [16]. Meanwhile however, two characteristic peaks of the Li_2TiO_3 phase around the 2θ angle of 20.0° gradually disappeared when the calcination temperature increased from 600 °C to 900 °C. With

increasing temperature, the long range ordering (LRO) degree of cations indicated by the intensity of (0 0 2) peak decreased and became almost completely disordered when the temperature was over 800 °C. The Li_2TiO_3 phase later changed from a monoclinic rock salt structure ($C2/c$ space group) to a cubic rock salt structure ($Fm\bar{3}m$ space group). Actually, Bian et al.[17] reported that $(1-y)Li_2TiO_3 + yMgO$ systems with rock salt structure ($0 \leq y \leq 0.5$) had a sequence of chemical reaction as follows:

$$\text{for } 0 \leq y \leq 0.3, (1-y)Li_2TiO_3 + yMgO \rightarrow Li_2TiO_3 \text{ (monoclinic } (C2/c)) \quad (2),$$

$$\text{and for } 0.4 \leq y, \ (1-y)Li_2TiO_3 + yMgO \rightarrow Li_2TiO_3 \text{ (cubic } (Fm\bar{3}m)) \quad (3).$$

As the calcination temperature increased from 900 °C to 1000 °C, one new phase, $Li_2Mg_3TiO_{63}$, was formed, and the MgO completely disappeared. This finding indicated further reactions between $Li_2Mg_zTiO_{3+z}$ ($z< 3$) and MgO. Furthermore, as temperature was increased to 1000 °C, peaks of Li_2TiO_3 phase shifted slightly to lower angles, and became the XRD patterns of the $Li_2Mg_3TiO_6$ phase. This finding was attributable to the substitution of larger Mg^{2+} (R= 0.72 Å) in place of smaller Li^+ and Ti^{4+} (R_{av}= 0.695 Å) [17, 18]. This finding implies a remarkable chemical reaction between the MgO and Li_2TiO_3 phases, which eventually form the $Li_2Mg_3TiO_6$ phase. When the samples were calcined from 1000 °C to 1200 °C, the samples' main phase exhibited the $Li_2Mg_3TiO_6$ cubic phase with rock salt structure in $Fm\bar{3}m$ space group (225), and the other phase was found to be $CaTiO_3$, which was indexed based on the JCPDS file 89-6949. As a result, the phase transition in $Li_2Mg_{3-x}Ca_xTiO_6$ system can be expressed as follows according to Fig. 1:

$$Mg(OH)_2 \bullet 4MgCO_3 \bullet 5H_2O \xrightarrow{25℃\sim400\ ℃} MgO \quad (4)$$

$$CaCO_3 \xrightarrow{400℃\sim500\ ℃} CaO \quad (5)$$

$$Li_2CO_3 + TiO_2 \xrightarrow{400\ ℃\sim500\ ℃} Li_2TiO_3 \text{ (monoclinic } (C2/c)) \quad (6)$$

$$Li_2TiO_3 \text{ (monoclinic } (C2/c)) + MgO \xrightarrow{600℃\sim800\ ℃} Li_2TiO_3 \text{ (monoclinic } (C2/c)) \quad (7)$$

$$Li_2TiO_3\ (\text{monoclinic}\ (C2/c)) + MgO \xrightarrow{800℃\sim900\ ℃} Li_2TiO_3\ (\text{cubic}\ (Fm\bar{3}m)) \quad (8)$$

$$CaO + TiO_2 \xrightarrow{700\ ℃\sim800\ ℃} CaTiO_3 \quad (9)$$

$$Li_2TiO_3(\text{cubic}\ (Fm\bar{3}m)) + MgO \xrightarrow{1000\ ℃\sim1200℃} Li_2Mg_3TiO_6\ (\text{cubic}\ (Fm\bar{3}m)) \quad (10)$$

Fig. 2 presents the powder XRD patterns of LMCxT (x=0.00~0.18) ceramics sintered at 1280 °C for 6 h in air. At x=0.00, the peaks of $Li_2Mg_3TiO_6$ were indexed as (1, 1, 1), (2, 0, 0), (2, 2, 0), (3, 1, 1), and (4, 0, 0). The spectra indicated a rock salt structure with $Fm\bar{3}m$ space group (225), which was similar to the $Li_2Mg_3SnO_6$ cubic phase (JCPDS#39-0932). When x was increased from 0.03 to 0.18, the $Li_2Mg_3TiO_6$ and $CaTiO_3$ phases were observed coexisting with each other and thus formed a stable composite phase system. Furthermore, intensity of $CaTiO_3$ was found to gradually increase with increasing Ca^{2+} contents. The formation of the second phase could be caused by the difficulty in substituting relatively large calcium ions (R= 1.34 Å) compared to magnesium ions (R= 0.72 Å). As discussed above, there was a great possibility that the $Li_2Mg_3TiO_6$ could form when the magnesium contents were deficient. Fig. 3 presents the powder XRD patterns of $Li_2Mg_{3-x}TiO_6$ (x=0.00, 0.04, 0.12, 0.18) ceramics sintered at 1280 °C for 6 h in air (a) and the characteristic peak of (220) for $Li_2Mg_{3-x}TiO_6$ phase of corresponding samples (b). We found that only the $Li_2Mg_3TiO_6$ phase in a $Fm\bar{3}m$ space group with cubic structure formed under the condition of Mg deficiency. As the Mg deficient content increased, the characteristic peaks were moving towards higher 2θ angles slightly, which was attributable to the decreasing contents of larger Mg^{2+} (R= 0.72 Å) ions. In our work, two stable compounds $Li_2Mg_{3-x}TiO_6$ (0.00~0.18) and $CaTiO_3$ formed through one synthetic process, and Li_2TiO_3 only reacted with MgO to form $Li_2Mg_3TiO_6$ phase even the Mg content is deficient in $Li_2Mg_{3-x}Ca_xTiO_6$ system. Hence, it was very reliable to control the phase composition by compositional ratios in LMCxT system.

Fig. 4 shows the SEM of thermally etched surface images of LMCxT (x=0.00~0.18) ceramics sintered at 1280 °C for 6 h with (a) x =0.00, (b) x =0.03, (c) x =0.06, (d) x =0.09, (e) x =0.12 (f) x =0.15, (g) x =0.18, and the backscattering electron image (BEI) of fractured surface for LMCxT with (h) x= 0.15. It can be observed that surface images of pure samples exhibited a porous structure, and the large pores were distributed on the grains or around the grain boundaries. It is highly common to observe the pores in the Li containing compounds because lithium is volatile and evaporates at elevated sintering temperatures (≥1000 ^{o}C), and even the pores can be observed inside the ceramics[9, 19]. However, a small amount of the second phase, which was randomly distributed in the holes and grain boundaries, was observed with x=0.03. From the SEM micrographs, two types of co-exhibited crystal growth can easily be detected, and the amount of the secondary phase increased along with the calcium ion concentration. As the Ca^{2+} concentrations grew to 0.15 and 0.18, almost no porosity in the compact microstructure of the ceramics could be observed. Typically, a fractured photograph of LMCxT with x= 0.15 showed a dense and compact microstructure, and the large grains and small grains could be observed which were considered as $Li_2Mg_3TiO_6$ and $CaTiO_3$ phase respectively. The decrease in the pores could be due to the presence of a small $CaTiO_3$ phase in the $Li_2Mg_3TiO_6$ ceramics. Similar results could also be observed in $Li_2ZnTi_{3+x}O_{8+2x}$ ceramics with extra TiO_2 phase and $Li_2A_{1-x}Ca_xTi_3O_8$ ceramics with a $CaTiO_3$ secondary phase.

EDX was employed to identify the chemical composition of two shaped grains shown in Fig. 4. Fig. 5 presents the EDX spectra of marked areas (A~G) of LMCxT ceramics corresponding to Fig. 4. The testing results are described in Table 1. As shown in Table 1 and Fig. 5, points A, B, C and E, representing the large grains, contained the elements Mg, Ti and O. However, points D and F, representing the small grains, included the elements Ca, Ti and O. The elements Mg, Ca, Ti and O were

found in area G. According to Table 1, the ratios of Mg: Ti were close to 3: 1, and the ratios of Ca: Ti were approximately 1: 1. Thus, the large grains should be the $Li_2Mg_3TiO_6$ phase, and small grains should be the $CaTiO_3$ phase. The two phases' co-existence in this system is consistent with the XRD results. Because the sintering temperature of the pure $CaTiO_3$ ceramic was about1,300~1,400 °C [20, 21], it was possible that the small $CaTiO_3$ grain size could be attributed to the relatively low sintering temperature. The optimal sintering temperature of the $Li_2Mg_3TiO_6$ ceramics was approximately 1,280 °C in this experiment.

Fig. 6 displays the (a) Apparent density, (b) Quality factor, (c) Dielectric constant and (d) Temperature coefficient of the resonant frequency of LMCxT (x= 0.00~0.18) as a function of the sintering temperature and Ca content. As shown in Fig. 6(a), apparent densities increased because of the densification process at a given concentration. This increase was followed by a slight decrease, which was attributed to the over-sintering process [22]. Furthermore, the optimal sintering temperature of LMCxT increased slightly from 1280 °C to 1280 °C when the Ca contents rose to 0.15, which may be contributed to the higher concentration of the $CaTiO_3$ phase. Meanwhile, the apparent densities increased remarkably from 3.29 g/cm^3 to 3.50 g/cm^3 with increasing $CaTiO_3$ content, which was caused by the increasing amount of $CaTiO_3$ phase (4.04 g/cm^3, JCPDS# 89-6949) and elimination of pores. It can be demonstrated by comparing the SEM images that the increased densification could be attributable to the elimination of pores in the ceramics.

The variation of the quality factor of LMCxT ceramics as a function of sintering temperature and calcium content is shown in Fig. 5(b). The change in Q×f value and apparent density varied similarly at a given calcium content. When the sintering temperature increased, the Q×f value of the ceramics initially increased and reached a maximum at their optimal sintering temperature and later declined as

the sintering temperature increased further. These changes were considered to correlate with the compactness of the samples; a higher Q×f value was usually related to a denser microstructure [23]. At the same time, however, a sustained downward trend in the Q×f value, decreasing from 148,713 GHz to 79,845 GHz, was observed as calcium content increased. The $CaTiO_3$ had a very low Q×f of approximately 3,600 GHz [24] compared to $Li_2Mg_3TiO_6$ ceramics. Therefore, the $CaTiO_3$ phase's lower Q×f was the reason for the sharp decrease in the Q×f of the $Li_2Mg_{3-x}Ca_xTiO_6$ ceramics.

Fig. 5(c) shows the change in the dielectric constant of LMCxT ceramics as a function of calcium content and sintering temperature. As sintering temperature increased, the dielectric constant only changed slightly at a given calcium content. This finding was observed because all samples showed high densification, and the dielectric constant showed limited dependence on the sintering temperature when samples were in high densification and compact microstructure [25]. However, the dielectric constant was highly correlated to the calcium content. In general, the dielectric constant is affected by density and the secondary phase [26]. Therefore, the increase in dielectric constant from 14.8 to 20.6 is reasonable because of the elimination of pores (ε_r=1) and the increasing amount of the $CaTiO_3$ phase (ε_r=170) [24].

Fig. 5(d) depicts the variation of the temperature coefficient at the resonant frequency and dielectric constant as a function of calcium content (x). The τ_f of $Li_2Mg_{3-x}Ca_xTiO_6$ increased significantly from −42.4 to +10.8 ppm/°C. It is well-known that the $CaTiO_3$ has a large positive τ_f of +800 ppm/◦C[21], and it is widely used to tune the τ_f of microwave dielectric ceramics, which have a highly negative τ_f. Hence, the high positive τ_f of the $CaTiO_3$ phase was the prime component of the increase in the τ_f of $Li_2Mg_{3-x}Ca_xTiO_6$ ceramics with increasing calcium content. As a result, a near zero τ_f value was obtained when x was 0.12, which was of great significance for this system. As clearly seen

from Fig. 5(d), both ε_r and τ_f increased linearly when the Ca content increased, which was probably explained by linear addition theory [27].

In summary, when the calcium content was 0.12, the LMCxT ceramics sintered at 1280°C for 6 h exhibited excellent comprehensive properties of ε_r= 17.8, Q×f= 102,246 GHz and τ_f = -0.7 ppm/°C. Furthermore, not only were the comprehensive microwave properties of LMCxT superior to that of the pure $Li_2Mg_3TiO_6$ ceramics [9], but LMCxT presented good relative densities and a compact microstructure, as well. In addition, Table 2 contains the microwave dielectric properties of some typical ceramics with a dielectric constant approximately 18. As shown in Table 2, our work had an obvious advantage in microwave dielectric and sintering properties over other high Q systems.

4. Conclusions

The influence of Ca-substitution for Mg on the sintering behaviors, phase structure, microstructure and microwave dielectric properties of $Li_2A_{3-x}Ca_xTiO_6$ were systematically investigated in this study. As the calcination temperature was 500 °C, the Li_2TiO_3 phase with monoclinic rock salt structure in C2/c space group started to form. As the samples were calcined from 600 °C to 900 °C, there was a remarkable chemical reaction between the MgO and the Li_2TiO_3 phase, which eventually formed the $Li_2Mg_3TiO_6$ phase. The XRD patterns indicated the $Li_2Mg_3TiO_6$ and $CaTiO_3$ co-existed with each other and formed a stable composite system when the calcium was added. The SEM photographs demonstrated that the pores caused by Li evaporation could be effectively reduced due to the appearance of $CaTiO_3$. The relative density and microwave dielectric properties were strongly dependent on the calcium content. As x increased from 0 to 0.18, the relative density was significantly improved due to the elimination of pores. As the intensity of the $CaTiO_3$ phase increased, the ε_r rose from 14.8 to 20.6; the Q×f decreased from

148,713 GHz to 79,845 GHz, and the τ_f increased significantly from −42.4 to +10.8 ppm/°C. At x=0.12, the LMCxT ceramics sintered at 1280 °C for 6 h exhibited excellent comprehensive properties of ε_r= 17.8, Q×f= 102,246 GHz and τ_f= -0.7 ppm/°C, which had an obvious advantage in microwave dielectric and sintering properties over other high Q systems.

Acknowledgments

This work is supported by the Open Foundation of National Engineering Research Center of Electromagnetic Radiation Control Materials (ZYGX2016K003-5) and by National Natural Science Funds of China (Grant No. 51402039).

References

[1] D. Zhou, W.-B. Li, H.-H. Xi, L.-X. Pang, G.-S. Pang, Phase composition, crystal structure, infrared reflectivity and microwave dielectric properties of temperature stable composite ceramics (scheelite and zircon-type) in $BiVO_4$–YVO_4 system, J. Mater. Chem. C. 3 (11) (2015) 2582-2588.

[2] S. George, M.T. Sebastian, Synthesis and Microwave Dielectric Properties of Novel Temperature Stable High Q, $Li_2ATi_3O_8$ (A=Mg, Zn) Ceramics, J. Am. Ceram. Soc. 93 (8) (2010) 2164-2166.

[3] M.T. Sebastian, Dielectric materials for wireless communication, Elsevier, 2010.

[4] D. Zhou, C.A. Randall, L.-X. Pang, H. Wang, J. Guo, G.-Q. Zhang, X.-G. Wu, L. Shui, X. Yao, Microwave Dielectric Properties of Li_2WO_4 Ceramic with Ultra-Low Sintering Temperature, J. Am. Ceram. Soc. 94 (2) (2011) 348-350.

[5] L.-X. Pang, D. Zhou, Microwave Dielectric Properties of Low-Firing Li_2MO_3 (M=Ti, Zr, Sn) Ceramics with B_2O_3–CuO Addition, J. Am. Ceram. Soc. 93 (11) (2010) 3614-3617.

[6] D. Zhou, C.A. Randall, H. Wang, L.-X. Pang, X. Yao, Microwave Dielectric Ceramics in Li_2O–Bi_2O_3–MoO_3 System with Ultra-Low Sintering Temperatures, J. Am. Ceram. Soc. 93 (4) (2010) 1096-1100.

[7] S. George, M.T. Sebastian, Microwave dielectric properties of novel temperature stable high Q Li2$Mg_{1-x}Zn_xTi_3O_8$ and $Li_2A_{1-x}Ca_xTi_3O_8$ (A = Mg, Zn) ceramics, J. Eur. Ceram. Soc. 30 (12) (2010) 2585-2592.

[8] Y. Zhao, P. Zhang, Microstructure and microwave dielectric properties of low loss materials $Li_3(Mg_{0.95}A_{0.05})_2NbO_6$ (A = Ca^{2+}, Ni^{2+}, Zn^{2+}, Mn^{2+}) with rock-salt structure, J. Alloy. Compd. 658 (2016) 744-748.

[9] H. Wu, E.S. Kim, Correlations between crystal structure and dielectric properties of high-Q materials in rock-salt structure Li_2O–MgO–BO_2 (B= Ti, Sn, Zr) systems at microwave frequency, RSC. Adv. 6 (53) (2016) 47443-47453.

[10] Z. Fu, P. Liu, J. Ma, X. Zhao, H. Zhang, Novel series of ultra-low loss microwave dielectric ceramics: $Li_2Mg_3BO_6$ (B = Ti, Sn, Zr), J. Eur. Ceram. Soc. 36 (3) (2016) 625-629.

[11] A. ávan Keulen, J. ávan Ommen, The role of tin in Li/Sn/MgO catalysts for the oxidative coupling

of methane, J. Chem. Soc., Chem. Commun. (21) (1992) 1546-1547.

[12] J.J. Bian, Y.F. Dong, Sintering behavior, microstructure and microwave dielectric properties of $Li_{2+x}TiO_3$ ($0 \le x \le 0.2$), Mater. Sci. Eng. B. 176 (2) (2011) 147-151.

[13] Y. Li, H. Li, J. Li, B. Tang, S. Zhang, H. Chen, Y. Wei, Effect of TiO_2 Ratio on the Phase and Microwave Dielectric Properties of $Li_2ZnTi_{3+x}O_{8+2x}$ Ceramics, J. Electron. Mater. 43 (4) (2014) 1107-1111.

[14] G. Subodh, M.T. Sebastian, Glass-Free $Zn_2Te_3O_8$ Microwave Ceramic for LTCC Applications, J. Am. Ceram. Soc. 90 (7) (2007) 2266-2268.

[15] Z. Fu, P. Liu, J. Ma, B. Guo, X. Chen, H. Zhang, Microwave dielectric properties of low-fired Li_2SnO_3 ceramics co-doped with MgO–LiF, Mater. Res. Bull. 77 (2016) 78-83.

[16] D. Wei, Y. Zhou, D. Jia, Y. Wang, Formation of $CaTiO_3/TiO_2$ composite coating on titanium alloy for biomedical applications, J. Biomed. Mater. Res. B. 84B (2) (2008) 444-451.

[17] J.J. Bian, Y.F. Dong, New high Q microwave dielectric ceramics with rock salt structures: $(1-x)Li_2TiO_3 + xMgO$ system ($0 \le x \le 0.5$), J. Eur. Ceram. Soc. 30 (2) (2010) 325-330.

[18] R.t. Shannon, Revised effective ionic radii and systematic studies of interatomic distances in halides and chalcogenides, Acta Crystallogr. Sect. A. 32 (5) (1976) 751-767.

[19] Y. Iida, Evaporation of Lithium Oxide from Solid Solution of Lithium Oxide in Nickel Oxide, J. Am. Ceram. Soc. 43 (3) (1960) 171-172.

[20] I.M. Reaney, P. Wise, R. Ubic, J. Breeze, N.M. Alford, D. Iddles, D. Cannell, T. Price, On the temperature coefficient of resonant frequency in microwave dielectrics, Philos. Mag. A. 81 (2) (2001) 501-510.

[21] T. Liu, X.Z. Zhao, W. Chen, A/B site modified CaTiO3 dielectric ceramics for microwave application, J. Am. Ceram. Soc. 89 (3) (2006) 1153-1155.

[22] X. Sha, Z. Lü, X. Huang, J. Miao, Z. Liu, X. Xin, Y. Zhang, W. Su, Influence of the sintering temperature on electrical property of the $Ce_{0.8}Sm_{0.1}Y_{0.1}O_{1.9}$ electrolyte, J. Alloy. Compd. 433 (1–2) (2007) 274-278.

[23] S.H. Yoon, G.-K. Choi, D.-W. Kim, S.-Y. Cho, K.S. Hong, Mixture behavior and microwave dielectric properties of $(1-x)CaWO_4–xTiO_2$, J. Eur. Ceram. Soc. 27 (8–9) (2007) 3087-3091.

[24] L. Li, X.M. Chen, X.C. Fan, Characterization of $MgTiO_3–CaTiO_3$-Layered Microwave Dielectric Resonators with TE01δ Mode, J. Am. Ceram. Soc. 89 (2) (2006) 557-561.

[25] J. Li, Y. Han, T. Qiu, C. Jin, Effect of bond valence on microwave dielectric properties of $(1-x)CaTiO3–x(Li0.5La0.5)TiO3$ ceramics, Mater. Res. Bull. 47 (9) (2012) 2375-2379.

[26] Y. Zhao, P. Zhang, High-Q microwave dielectric ceramics using Zn3Nb1.88Ta0.12O8 solid solutions, J. Alloy. Compd. 662 (2016) 455-460.

[27] D. Zhou, D. Guo, W.-B. Li, L.-X. Pang, X. Yao, D.-W. Wang, I.M. Reaney, Novel temperature stable high-ε_r microwave dielectrics in the $Bi_2O_3–TiO_2–V_2O_5$ system, J. Mater. Chem. C. 4 (23) (2016) 5357-5362.

[28] R.C. Pullar, J. Breeze, N. Alford, Microwave dielectric properties of columbite-structure niobate ceramics, $M^{2+}Nb_2O_6$, Key Eng. Mater. 224 (2002) 1-4.

[29] K. Surendran, P. Bijumon, P. Mohanan, M. Sebastian, (1-x) $MgAl_2O_4$-$xTiO_2$ dielectrics for microwave and millimeter wave applications, Appl. Phys. A. 81 (4) (2005) 823-826.

[30] R.C. Pullar, J.D. Breeze, N.M. Alford, Characterization and Microwave Dielectric Properties of $M^{2+}Nb_2O_6$ Ceramics, J. Am. Ceram. Soc. 88 (9) (2005) 2466-2471.

[31] C.-L. Huang, J.L. Hou, C.-L. Pan, C.-Y. Huang, C.-W. Peng, C.-H. Wei, Y.-H. Huang, Effect

of ZnO additive on sintering behavior and microwave dielectric properties of $0.95MgTiO_3$–$0.05CaTiO_3$ ceramics, J. Alloy. Compd. 450 (1–2) (2008) 359-363.

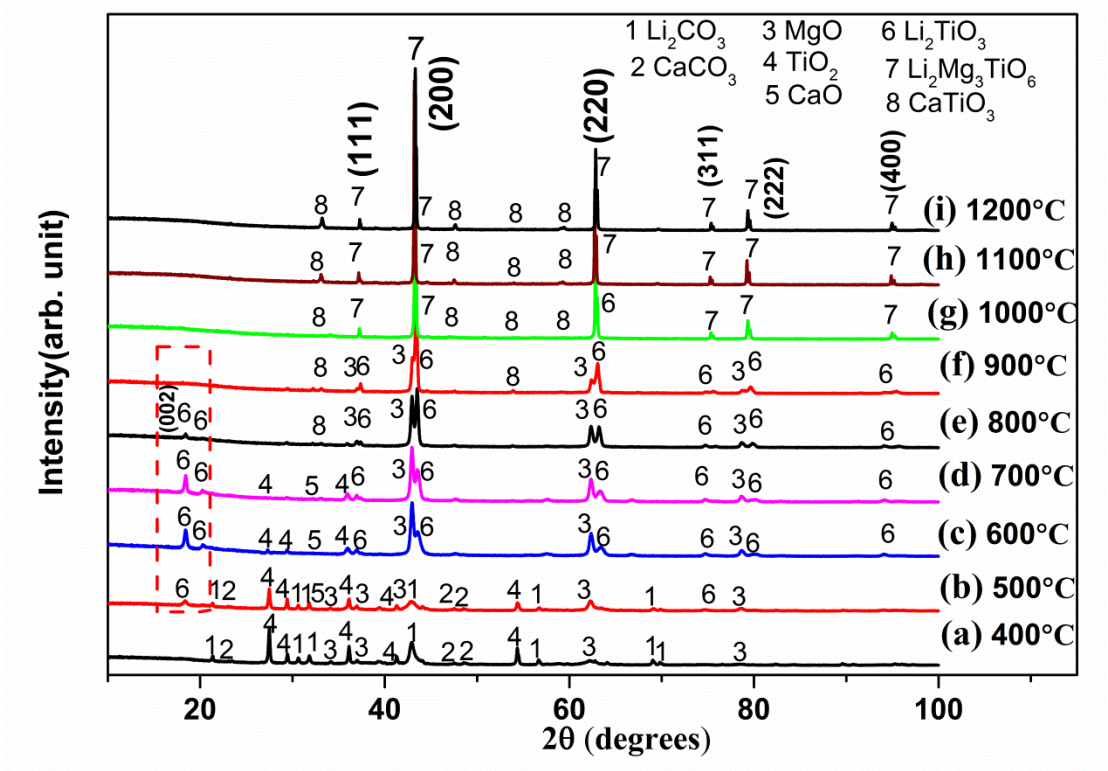

Fig. 1. XRD patterns of $Li_2Mg_{3-x}Ca_xTiO_6$ (x=0.12) powders calcined at (a) 400 °C, (b) 500 °C,(c) 600 °C, (d) 700 °C (e) 800 °C (f) 900 °C (g) 1000 °C (h) 1100 °C and (i) 1200 °C for 4 h in air

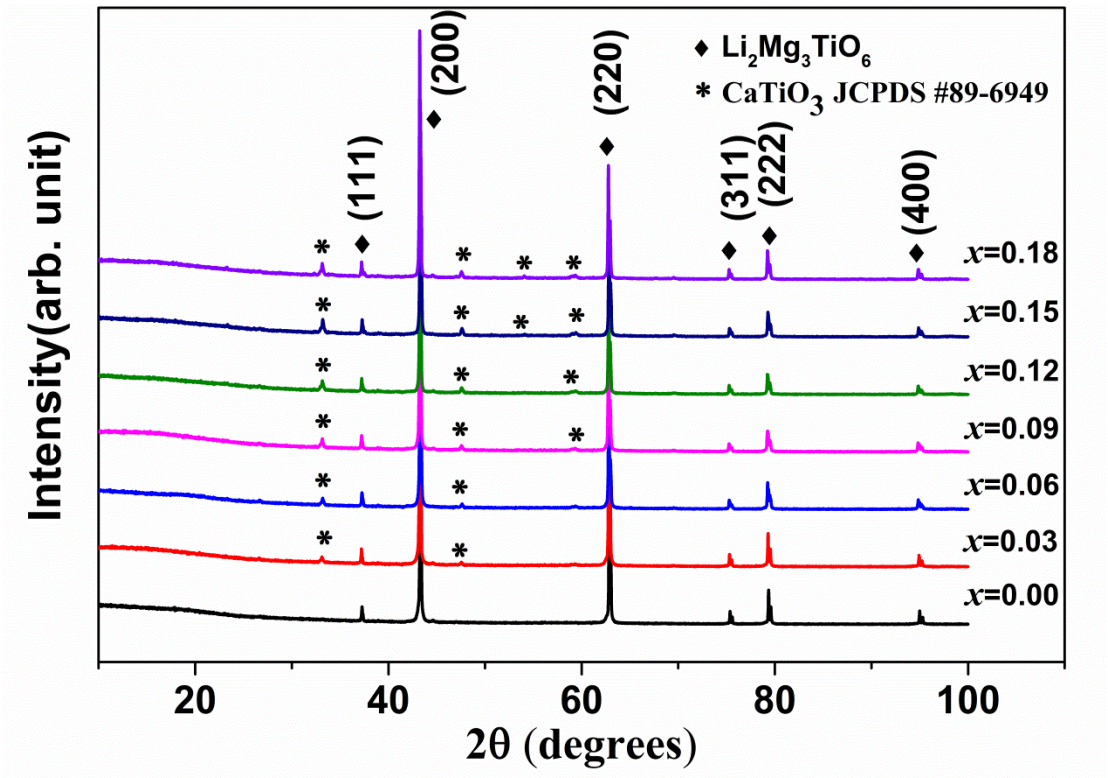

Fig. 2. Powder XRD patterns of $Li_2Mg_{3-x}Ca_xTiO_6$ (x=0.00~0.18) ceramics sintered at 1280 °C for 6 h in air.

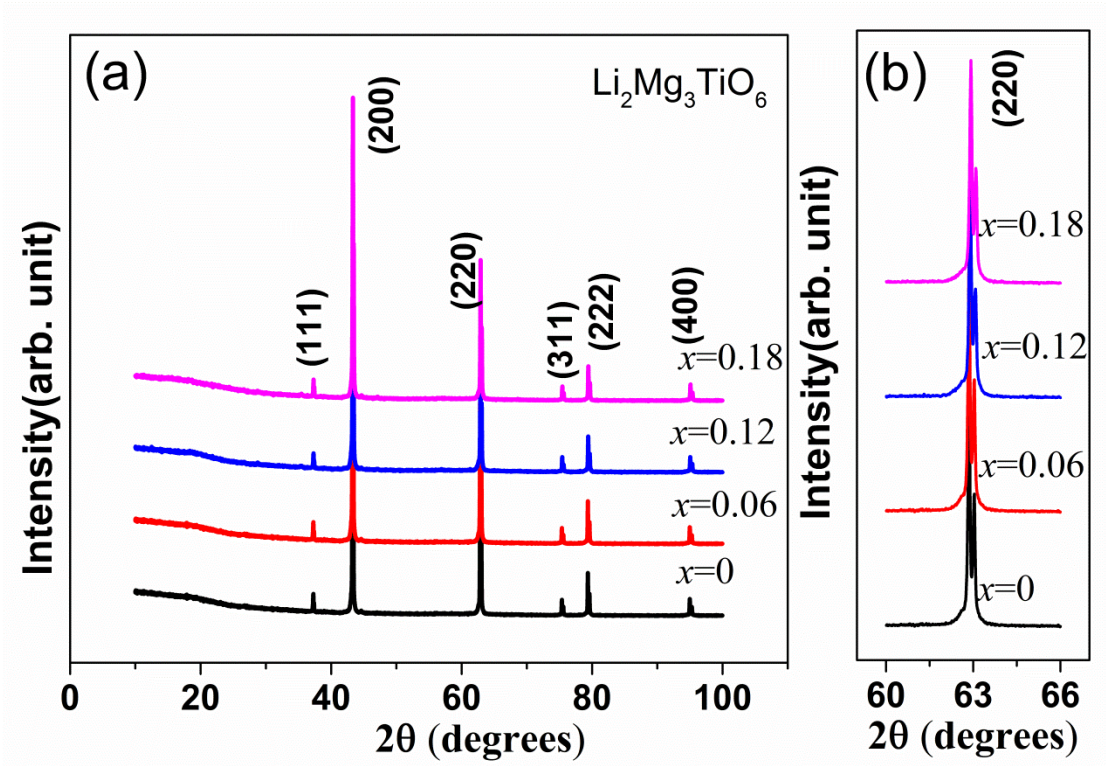

Fig. 3. (a) Powder XRD patterns of $Li_2Mg_{3-x}TiO_6$ (x=0.00~0.18) ceramics sintered at 1280 °C for 6 h in air; (b) the characteristic peaks of (220) for $Li_2Mg_{3-x}TiO_6$ phase of corresponding samples

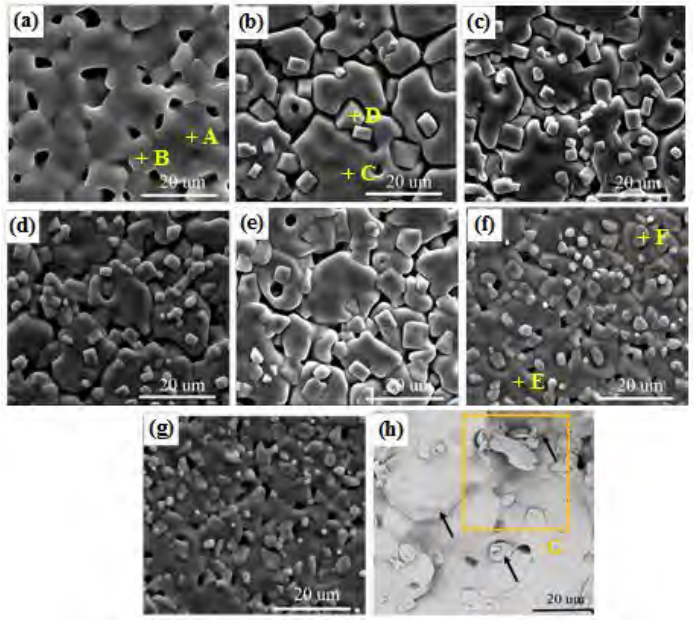

Fig. 4. SEM of thermally etched surface images of $Li_2Mg_{3-x}Ca_xTiO_6$ (x=0.00~0.18) ceramics sintered at 1280 °C for 6 h with (a) x =0.00, (b) x =0.03, (c) x =0.06, (d) x =0.09, (e) x =0.12 (f) x =0.15 and (g) x =0.18, and backscattering electron image (BEI) of fractured surface for LMCxT with (h) x= 0.15.

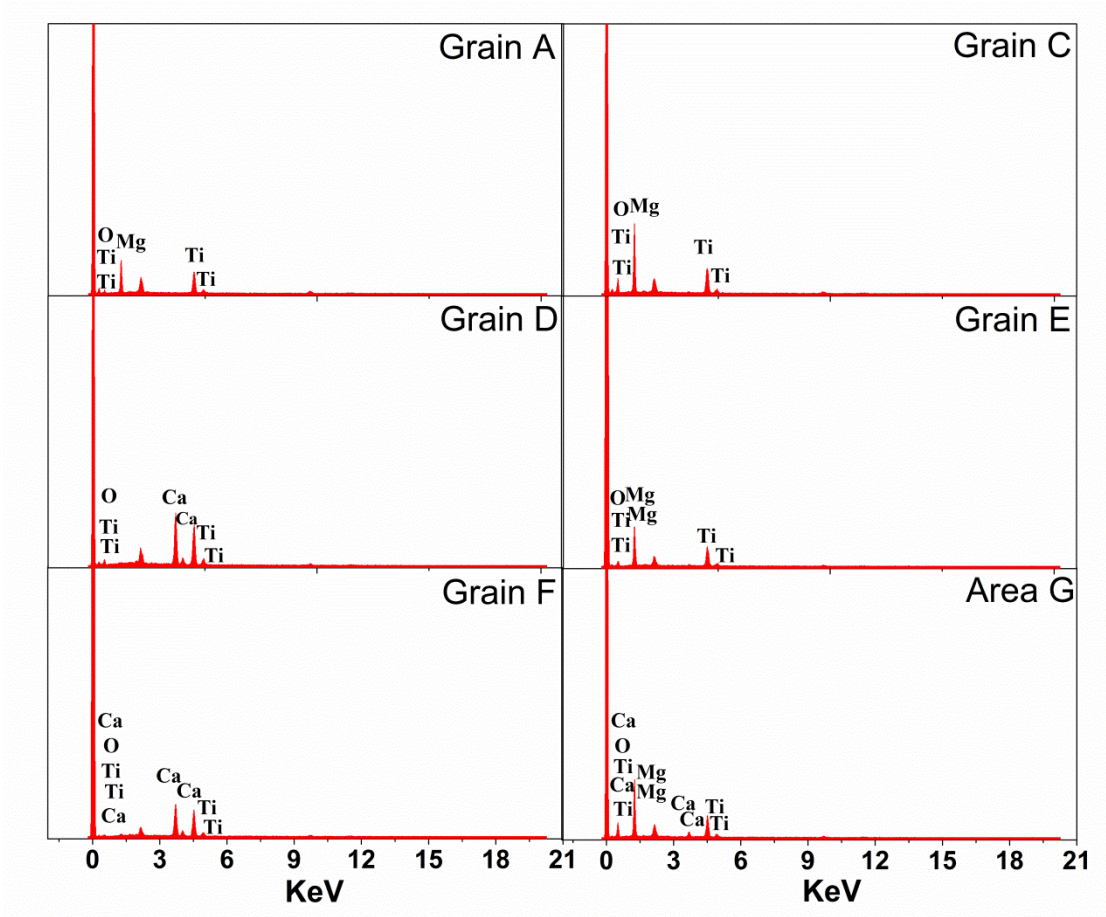

Fig. 5. EDX analysis on the marked areas of $Li_2Mg_{3-x}Ca_xTiO_6$ ceramics sintered at 1280 °C corresponding to Fig. 4.

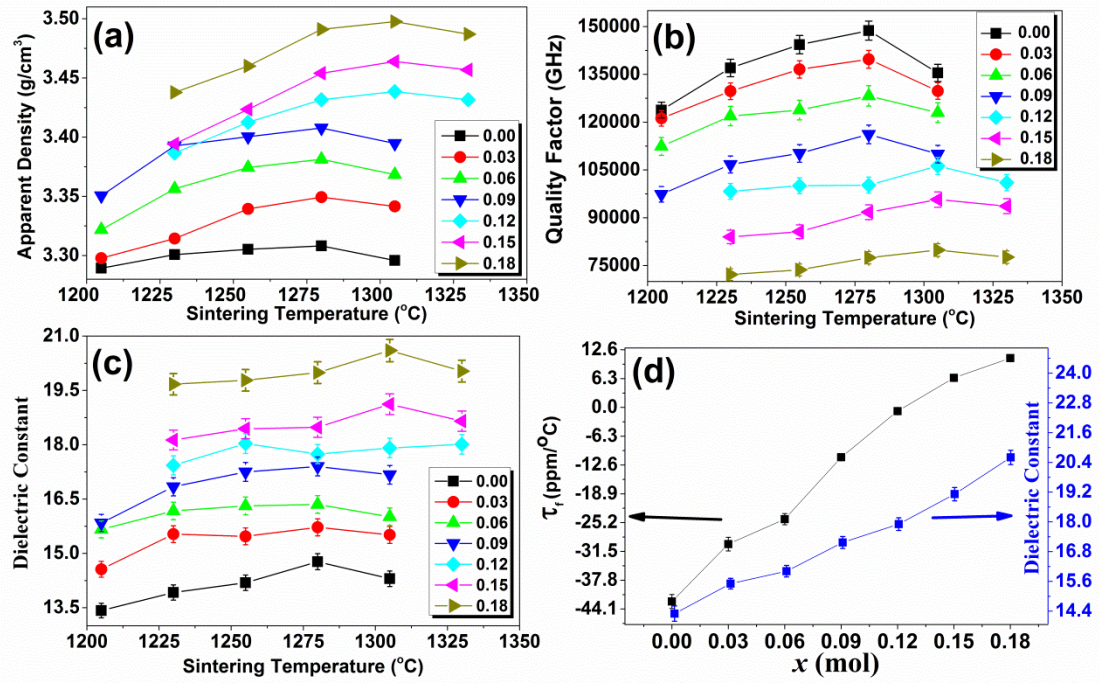

Fig. 6. (a) Apparent density, (b) Quality factor (c) Dielectric constant and (d) Temperature coefficient of resonant frequency of LMC_xT (x= 0.00~0.18) sintered at 1205-1330 °C for 6 h.

Table 1 The energy dispersive X-ray analysis (EDX) data of LMCxT ceramics marked in Fig. 3.

Spot	Atom (%)				
	Mg	Li	Ca	Ti	O
A	35.37	--	--	13.71	50.92
B	32.56	--	--	12.12	55.32
C	33.24	--	--	12.42	54.34
D	--	--	21.32	24.05	54.63
E	39.37	--		15.62	41.01
F	--	--	24.17	26.38	49.55
G	29.41	--	4.95	10.99	54.65

Table 2 The microwave dielectric properties of some typical ceramics when dielectric constant was approximately 18.

Ceramics composition	Sintering temperature(°C)	ε_r	Q×f (GHz)	τ_f(ppm/°C)	Reference
$MgTiO_3$	1400	17	110,000	-54	[28]
$Li_2Mg_{2.88}Ca_{0.12}TiO_6$	1305	17.8	102,246	-0.7	This work
$5MgO-Ta_2O_5-TiO_2$	1560	18	118,000	-56	[29]
$MgNb_2O_6$	1300	18.4	79600	-65	[30]
$0.95MgTiO_3$-05$CaTiO_3$ +0.25wt%V_2O_5	1300	18.9	69,000	-10.7	[31]